Comparison between Electron Beam and Near-Field Light on the Luminescence Excitation of GaAs/AlGaAs Semiconductor Quantum Dots

Tadashi MITSUI, Takashi SEKIGUCHI, Daisuke FUJITA[1] and Nobuyuki KOGUCHI[1]

Nanomaterials Laboratory, National Institute for Materials Science, Namiki 1-1, Tsukuba, Ibaraki 305-0044, Japan
[1]*Nanomaterials Laboratory, National Institute for Materials Science, Sengen 1-2-1, Tsukuba, Ibaraki 305-0047, Japan*

To precisely estimate electron beam excitation intensity and to understand exactly the electron beam excitation process in a semiconductor, we observed and compared the luminescence properties of GaAs/Al$_{0.3}$Ga$_{0.7}$As self-assembled quantum dots (QDs) by the cathodoluminescence (CL) and near-field scanning optical microscopy (NSOM) techniques. The actual excitation densities measured by the CL and NSOM techniques are nearly equal at the dose rates considered, except for a low dose rate in which the actual excitation density measured by the CL technique is slightly larger than that measured by NSOM technique. However, the difference between these excitation densities is extremely small relative to the expected value when electron–hole (e–h) pairs are temporarily densified as a result of a cascade process. Therefore, the spatially inhomogeneous distribution of e–h pairs in the generation and diffusion regions is considered to be the main cause of the small difference in excitation density in such a case.   [DOI: 10.1143/JJAP.44.1820]

KEYWORDS: cathodoluminescence, quantum dots, near-field scanning optical microscopy, excitation, electron–hole pair

1. Introduction

Techniques for observing localized luminescence properties in semiconductors are very important not only for the study of semiconductor physics but also for the development of optoelectronic devices. Cathodoluminescence (CL)[1–4] is a powerful tool for such observation because it has very convenient features for carrying out experiments, such as a large scanning area and a short total measuring time. By using the CL technique, we can observe any point on a sample because an electron beam can scan a large area more easily than piezo-driving devices. Moreover, since the excitation intensity of an electron beam is significantly larger than that of light, the luminescence intensity measured by the CL technique is high in general. This high intensity reduces exposure time, thus experimental results are delivered faster. However, the high excitation intensity sometimes causes the degradation of both the energy and the spatial resolution. Thus, precision is important in estimating electron beam excitation intensity and in understanding the electron beam excitation process.

Luminescence emission from a semiconductor is caused by the recombination of an electron–hole (e–h) pair generated by an electron beam or incident light. In the excitation process by light, the process is simple, because each photon generates only one e–h pair. Therefore, the properties of light such as wavelength (energy) or polarization directly affect the phenomenon of the e–h pair generation. In addition, the excitation intensity is temporally and spatially homogeneous in the generation region. Thus, we can reduce the excitation intensity to a level at which only one e–h pair exists in the generation region at any one moment, because the excitation intensity is highly proportional to the intensity of the incident light upon light excitation. On the other hand, the excitation process by an electron beam is complex, and is different from that by light. In the excitation process by an electron beam, the incident electron does not generate an e–h pair directly. Rather, the incident electron induces the X-ray emission by an inner-shell excitation process, the electron emission by an Auger effect, the secondary electron emission by a cascade process,

and so on. Because the Auger electrons generated at the first stage cause other Auger effects, the number of Auger electrons markedly increases. On the other hand, the secondary electron emission is induced by the collision between an incident electron and a valence electron, and secondary electrons also increase in number. Lastly, each incident electron in the cascade process generates about 1×10^3 secondary electrons, although the ratio of the Auger effect to the collision process is not precisely determined. In the case of the electron beam of few keV energy used in scanning electron microscopy (SEM), the X-ray emission by the inner-shell excitation process is inferior to the electron emission by the Auger effect.

Figure 1 shows a schematic illustration of the cascade process. The secondary electrons have kinetic energies of about 5–10 eV; they are excited and diffused in a spherical region. The depth and diameter of the diffusion region are nearly equal, and the depth L_R is given by[5]

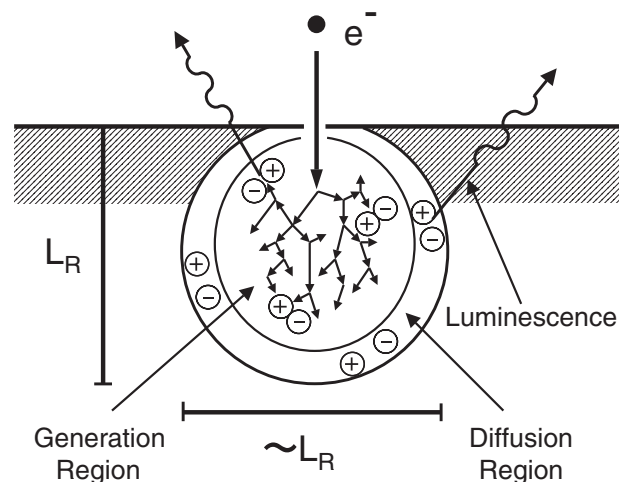$$L_R(\mu m) = \frac{0.0276A \cdot E^{\frac{5}{3}}}{\rho \cdot Z^{\frac{8}{9}}}, \tag{1}$$

Fig. 1. Schematic representation of cascade process in semiconductor by accelerated electron.

where A, Z, ρ, and E are the mass number, the atomic number, the volume density in g/cm^3, and the acceleration voltage of the electron beam in keV, respectively. The depth L_R becomes a few hundred nanometers for a general semiconductor sample with an electron beam of few keV. The e–h pairs generated by the secondary electrons recombine in the generation and diffusion regions, thus emitting luminescent light. Then, the spatial resolution of the CL technique is nearly equal to this L_R. Using this high spatial resolution, Petersson *et al.* characterized uncapped GaN dots on an AlGaN barrier material grown by metal-organic chemical vapor deposition.[6]

As we have shown, the mechanism by which an electron beam generates e–h pairs is more complex than that by light generation. Therefore, in order to estimate the excitation intensity and to understand the mechanism precisely, it is useful to compare the luminescence properties generated by electron beam excitation with those generated by light excitation. Ohno and Takeda have developed an *in situ* PL and CL measurement system using transmission electron microscopy (TEM), and have examined the spatial distribution of extended defects and point-defect complexes in chemical vapor deposition diamond.[7] However, the luminescence properties in a nanoscale region have not been estimated precisely. In order to compare the properties under the same excitation condition, in which the diameter of the generation region is a few hundred nanometers ($\sim L_R$), we used near-field scanning optical microscopy (NSOM)[8–13] to characterize the localized luminescence properties generated by light excitation. In the NSOM technique, a small aperture formed on the top of an optical fiber probe limits the generation region, allowing us to observe the properties of nanoscale structures such as semiconductor quantum dots (QDs).[14–16]

Semiconductor QDs have zero-dimensional structures in which electrons and holes are confined in all three dimensions, so that their densities of states become discrete. These states created by this marked phenomenon emit luminescence spectra consisting of well-isolated lines with narrow energy ranges in full width at half maximum (FWHM). These well-isolated, narrow lines are useful for characterizing the luminescence properties from the spectral viewpoint. Saiki and coworkers observed that such luminescence peaks originate from the ground-state excitons of InGaAs QDs, and that the peaks originating from upper excitation states and a biexciton state appear gradually as excitation density increases.[17,18] If many excitons exist in a small and confined region, they combine with each other. Because the energy of multicombined excitons is smaller than that of the quantum effect of QDs, multicombined exciton peaks appear very near the single exciton peak in the spectrum. Since these multicombined exciton peaks are also attributed to the same QDs, we consider these peaks as part of the luminescence peaks emitted by the QDs. Thus, the FWHM of the luminescence peaks reflects the number of excitons, and we can use it as an indicator of excitation density.

In this study, we estimate the excitation intensity of an electron beam and that of light by comparing the luminescence properties emitted from the discrete states of GaAs/AlGaAs QDs by the CL and NSOM techniques. Since there
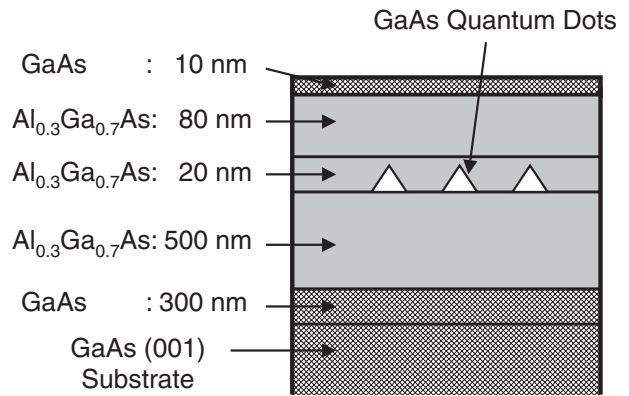

Fig. 2. Structure of GaAs/AlGaAs self-assembled quantum dots (QDs) used in this study. The samples were grown by modified droplet epitaxy. The diameter of each QD is about 20 nm.

are several intermediate processes, the excitation process by an electron beam is complex. Therefore, we disregard such intermediate processes, and only discuss the excitation density of e–h pairs at a certain dose rate by measuring the luminescence properties. We use the FWHM of the luminescence peaks as an indicator of excitation density because it is difficult to estimate the excitation density in a region of few hundred nanometers precisely.

2. Experiment

The samples used in this study were GaAs/$Al_{0.3}Ga_{0.7}As$ self-assembled QDs grown by modified droplet epitaxy (MDE).[19–21] Figure 2 shows the sample structure. A 300-nm-thick GaAs buffer layer and a 500-nm-thick GaAs/$Al_{0.3}Ga_{0.7}As$ barrier layer were grown at 580°C on a GaAs (001) wafer (p-type [Zn] $\sim 10^{18}$ cm^{-3}) after the native oxides were desorbed. Then the substrate temperature was reduced to 300°C. Ga droplets were deposited by a Ga molecular beam without an As flux. The total amount of Ga supplied was equal to 1.75 monolayers. Next, an As$_4$ molecular beam was irradiated on the sample surface, forming GaAs microcrystals. After an $Al_{0.3}Ga_{0.7}As$ barrier layer with a thickness of about 20 nm was grown at the same temperature, the sample was again heated to 580°C. We grew an 80-nm-thick $Al_{0.3}Ga_{0.7}As$ barrier layer. After the sample was annealed at 650°C for a few minutes, we grew a 10-nm-thick GaAs cap layer. The QD size was measured by SEM using the specimen without an 80-nm-thick barrier layer and that with a capping layer grown under the same conditions described above. The QD diameter was about 20 nm; the QD density of 6×10^9 cm^{-2} corresponded to 60 dots per μm^2.

For CL measurements, a specially designed system employing SEM (S-4200SE; Hitachi, Ltd., Tokyo, Japan) was used. The basic form of this system has been described in detail elsewhere.[22] The system had a high and homogeneous light-collection efficiency from a large sample area. Luminescent light from the sample was collected by an ellipsoidal mirror and guided to a detection unit through an optical fiber. A monochromator system (TRIAX 320; Jobin Yvon, S.A., France) recorded CL spectra. All CL data in this study were obtained at 20 K with an electron beam energy of 3 keV. Using eq. (1), in the case of an $Al_{0.3}Ga_{0.7}As$ sample,

the depth L_R becomes 117 nm. We used this value in the present study because it is nearly equal to the distance between each QD and the specimen surface, and because it approximates the aperture diameter of a conventional NSOM fiber probe.

For NSOM measurements, a high-sensitivity double-tapered fiber probe[23] was used (NFS-320; JASCO, Ltd., Tokyo, Japan). The sample was illuminated with a YAG-SHG laser ($\lambda = 532$ nm: 2.33 eV) through the aperture of the fiber probe. The energy of 2.33 eV corresponded to the condition under which the excitation energy exceeds the barrier band gap of 1.94 eV in our samples. In the measurement, the fiber probe was maintained constantly at 10 nm above the specimen surface by shear-force feedback control. The PL light was collected by the same aperture (illumination-collection (I-C) hybrid mode) to maintain the spatial resolution constant, and to prevent the influence of carrier diffusion. The PL light was guided into a monochromator and detected by a charge-coupled device. All NSOM data in this study were obtained at 15 K.

3. Results

Figure 3(a) shows the CL spectrum emitted from a GaAs/AlGaAs self-assembled QD sample obtained with an electron current of 50 pA. The spectrum was obtained with an energy resolution of 2.4 meV as the beam scanned a 2×2 μm square area. The spectrum indicates an AlGaAs barrier-layer peak at the energy of 1.91 eV with a shoulder.

More than ten QD peaks are present between 1.52 eV to 1.84 eV. This indicates that multiple QDs were excited simultaneously.

In order to characterize the QD peaks more precisely, we observed the PL spectra by NSOM with different excitation densities, ranging from 2.3 W/cm² to 14 W/cm². Figure 3(b) shows the PL spectra of an individual QD in the same specimen. The energy resolution of the spectra was 0.45 meV, and the aperture diameter of the probe was 200 nm. The spectra indicate a peak with the FWHM of 0.7 meV at the energy of 1.6480 eV (calculated value), and another at 1.6468 eV (1.2 meV below the main peak). The emission intensity of the latter peak decreases as the excitation density is reduced. From the energetic position and the excitation density dependence, this emission peak can be attributed to the recombination of biexcitons.[24] The FWHM of the peak at the energy of 1.6480 eV does not decrease even when the excitation density decreases to less than 2.3 W/cm². Therefore, the FWHM should be the intrinsic value of this QD.

To estimate the excitation intensity of the electron beam, we observed the FWHM of the peak using the CL and NSOM techniques with different excitation densities. Figure 4(a) shows the CL spectra of the other QD in another region of the same specimen obtained with the different electron currents indicated in the figure. The spectra were
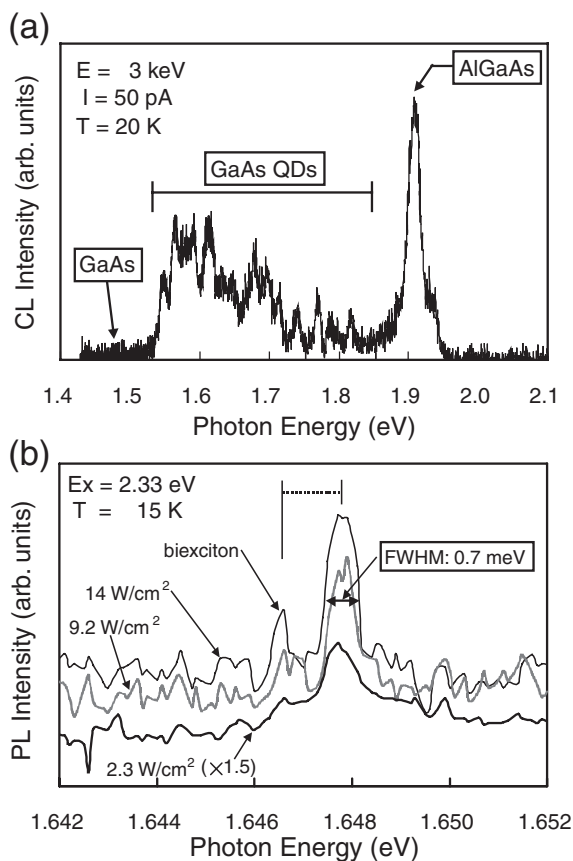

Fig. 3. CL and PL spectra of GaAs/AlGaAs self-assembled QD samples: (a) CL spectrum in wide energy range at 50 pA, (b) PL spectra obtained by NSOM with excitation densities of 2.3–14 W/cm².
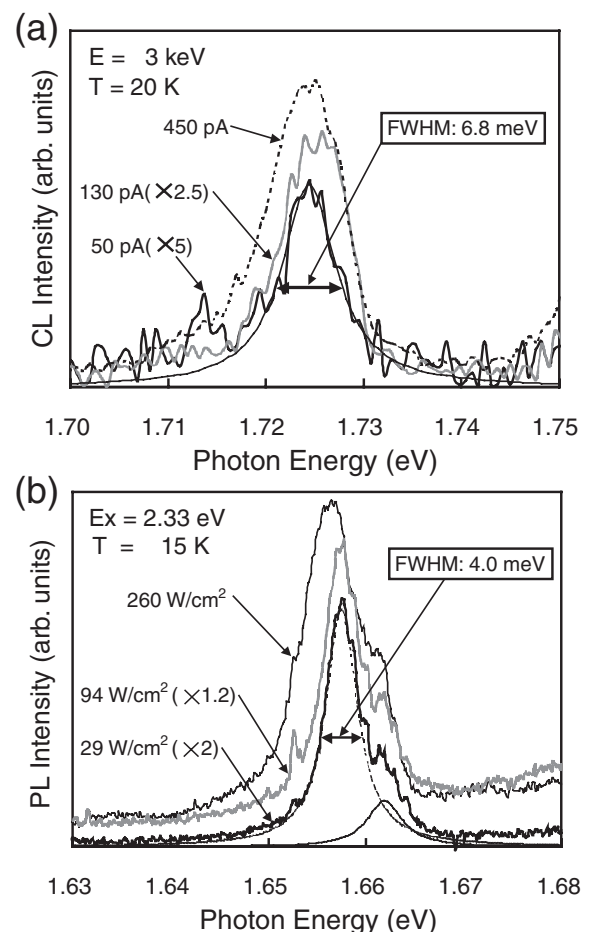

Fig. 4. CL and PL spectra of GaAs/AlGaAs self-assembled QDs with different excitation densities: (a) CL and (b) NSOM.

obtained without beam scanning, and the beam was irradiated near the individual QD. In these spectra, the energy resolution was 0.59 meV. The spectra indicate a peak at the energy of 1.724 eV, and the FWHM of the peak decreases with decreasing beam current. Here, we fitted a solid line to the luminescence peak of 50 pA using a Lorentzian function; 50 pA was the weakest current in this study. The FWHM of this peak was 6.8 meV.

Figure 4(b) shows the PL spectra of the other two QDs obtained with the excitation densities of 29 W/cm² to 260 W/cm². The excitation energy and the energy resolution were the same as in Fig. 3(b). The aperture diameter of the probe was 110 nm, approximately the diameter of the diffusion region in Fig. 4(a). The spectra indicate a peak at the energy of 1.658 eV with a shoulder; this peak becomes sharper as the excitation density is reduced. For 29 W/cm², we fitted the luminescence peak and the shoulder using Lorentzian functions centered at 1.658 eV and 1.661 eV, as shown by the broken and solid lines, respectively. The FWHM of the main peak was determined to be 4.0 meV.

Before concluding this section, we should note that there is no peak shift at the CL spectra indicated in Fig. 4(a) with different electron currents. We cannot find any peak shift in the emission peak of the barrier layer. Moreover, another experiment using a GaAs wafer also shows that there is no peak shift. These results suggest that the temperature does not change around the diffusion region, and that the local heating does not happen in the excitation densities considered.

4. Discussion

Before comparing the electron beam excitation with the light excitation, we consider again the excitation density in the cascade process. When a secondary electron generates an e–h pair in a semiconductor, such an electron requires a kinetic energy of about three times the band-gap energy.[25] Supposing that all the kinetic energy of one incident electron is used for the generation of e–h pairs, the multiplication factor is given by

$$C_{Amp} = \frac{1}{3} \cdot \frac{E}{E_g}, \tag{2}$$

where E and E_g are the electron beam energy and band-gap energy, respectively. On the other hand, the number of incident electrons entering a specimen per second is given by

$$N_{enter} = \frac{I}{e}, \tag{3}$$

where I and e are the beam current and the elementary electric charge, respectively. Using these two values, the number of e–h pairs generated per second in the diffusion region N_{e-h} is given by

$$N_{e-h} = C_{Amp} \cdot N_{enter} = \frac{1}{3} \cdot \frac{E}{E_g} \cdot \frac{I}{e} \quad (Number/s). \tag{4}$$

Because the recombination rate T is the reciprocal of the ground state emission lifetime τ, the number of e–h pairs existing in the generation and diffusion regions at the same time is given by

$$\frac{N_{e-h}}{T} = \frac{1}{3} \cdot \frac{E}{E_g} \cdot \frac{I}{e} \cdot \frac{1}{T} = \frac{1}{3} \cdot \frac{E}{E_g} \cdot \frac{I}{e} \cdot \tau \quad (Number). \tag{5}$$

Since the band-gap energy of the barrier layer in our sample is 1.94 eV, the electron beam energy and current are 3 keV and 50 pA, respectively, and the typical lifetime is 400 ps,[2] we determined that about 64 e–h pairs exist in the generation and diffusion regions at the same time. As mentioned earlier, in our sample, the diameter of the diffusion region became 117 nm and the QD diameter was about 20 nm. Therefore, the average number of e–h pairs in a QD is smaller than that obtained even when the multiplication factor used is maximum. Under actual excitation conditions, the e–h pairs are trapped by and are accumulated in QDs. Thus, the observed emission lines are expected to originate not only from the recombination of ground-state excitons, but also from that of multicombined excitons, and the FWHM is expected to reflect the excitation density, unlike the case shown in Fig. 3(b).

Keeping this in mind, we compared the excitation densities measured by the CL technique with those measured by the NSOM technique. Figure 5 plots the FWHMs measured by the NSOM and CL techniques as a function of actual dose rate. In the CL technique, we converted the electron beam current into the dose rate using the following equation, in which we assumed that the excitation density is homogeneous within the diffusion region.

$$D_{ex}(W/cm^2) = \frac{V \cdot I}{\pi \cdot (L_R/2)^2} \cdot \frac{1}{3} \tag{6}$$

Here, V is the acceleration voltage of the electron beam. As mentioned above, a factor of 3 is the coefficient whereby a secondary electron generates an electron–hole pair.[25] This plot indicates that the FWHMs measured by the CL and NSOM techniques are nearly equal at the actual dose rates considered, except for the FWHM measured by the CL technique at 470 W/cm². The FWHM of 6.8 meV measured by the CL technique is slightly larger than that of about 2 meV measured by the NSOM technique. Such an FWHM
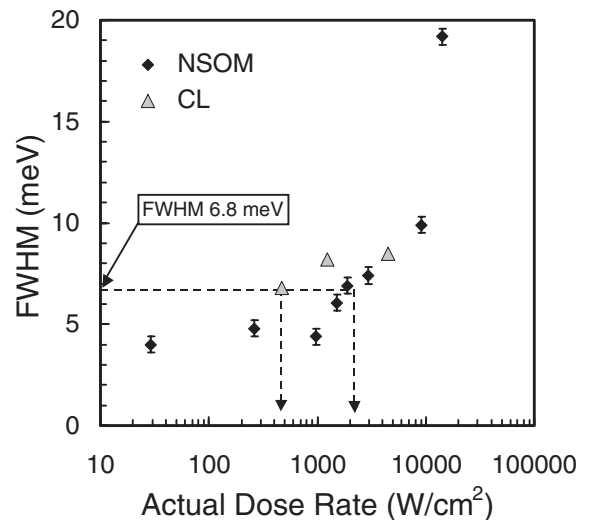

Fig. 5. Relationship between FWHM and excitation density of luminescence emitted from GaAs/AlGaAs QD. The FWHM of CL at 470 W/cm² is 6.8 meV.

measured by the CL technique corresponds to an excitation density of about $2\,\mathrm{kW/cm^2}$ measured by the NSOM technique. As mentioned earlier, because the excitation intensity of light is proportional to the intensity of incident light, this result suggests that the excitation intensity of the electron beam is not proportional to the dose rate. Note that the actual excitation density measured by the CL technique is only four times larger than the expected value estimated from the dose rate. Here, there are two possible reasons. Because the cascade process caused by an accelerated electron finishes within a few femtoseconds, the density of the e–h pairs is expected to increase temporarily. However, in such a case, the actual excitation density is expected to be extremely large to match the expected value estimated from the dose rate. This is because a few femtoseconds is about 1×10^5 times shorter than the ground-state emission lifetime of the QDs. On the other hand, supposing that there is a spatially inhomogeneous distribution of e–h pairs in the diffusion region, the luminescence property of QDs reflects the distribution in the diffusion region, since the diameter of the QDs is smaller than that of the diffusion region. In such a case, the excitation density increases when the electron beam irradiates near the QDs, because the e–h pairs diffuse from the center of the diffusion region. However, the difference is expected to be about ten times at most. Therefore, the spatially inhomogeneous distribution of e–h pairs is considered to be the main cause of the small difference.

5. Conclusion

To estimate the excitation intensity of an electron beam and that of near-field light, we have observed and compared the luminescence properties of GaAs/AlGaAs QDs by the CL and NSOM techniques. The actual excitation densities measured by the CL and NSOM techniques are nearly equal at the dose rates considered, except for a low dose rate of $470\,\mathrm{W/cm^2}$. At such a low dose rate, the excitation density measured by the CL technique is only four times larger than that measured by the NSOM technique. However, this value is too small if the temporally densification of e–h pairs resulting from the cascade process is the main cause of the difference in excitation density. Therefore, the difference is considered to reflect the spatial inhomogeneity of e–h pairs in the diffusion region.

1) P. M. Petroff, R. A. Logan and A. Savage: Phys. Rev. Lett. **44** (1980) 287.
2) B. G. Yacobi and D. B. Holt: J. Appl. Phys. **59** (1986) R1.
3) N. Yamamoto, J. C. H. Spence and D. Fathy: Philos. Mag. B **49** (1984) 609.
4) R. J. Graham, F. Shaapur, Y. Kato and B. R. Stoner: Appl. Phys. Lett. **65** (1994) 292.
5) K. Kanaya and S. Okayama: J. Phys. D **5** (1972) 43.
6) A. Petersson, A. Gustafsson, L. Samuelson, S. Tanaka and Y. Aoyagi: Appl. Phys. Lett. **74** (1999) 3513.
7) Y. Ohno and S. Takeda: Rev. Sci. Instrum. **66** (1995) 4866.
8) D. W. Pohl, W. Denk and M. Lanz: Appl. Phys. Lett. **44** (1984) 651.
9) U. Durig, D. W. Pohl and F. Rohner: J. Appl. Phys. **59** (1986) 3318.
10) A. Lewis, M. Isaacson, A. Harootunian and A. Muray: Ultramicroscopy **13** (1984) 227.
11) A. Harootunian, E. Betzig, M. Isaacson and A. Lewis: Appl. Phys. Lett. **49** (1986) 674.
12) E. Betzig, M. Isaacson and A. Lewis: Appl. Phys. Lett. **51** (1987) 2088.
13) E. Betzig, J. K. Trautman, T. D. Harris, J. S. Weiner and R. L. Kostelak: Science **251** (1991) 1468.
14) Y. Arakawa and H. Sakai: Appl. Phys. Lett. **40** (1982) 939.
15) T. Kuroda, S. Sanguinetti, M. Gurioli, K. Watanabe, F. Minami and N. Koguchi: Phys. Rev. B **66** (2002) 121302R.
16) H. Kamada, J. Temmyo, M. Notomi, T. Furuta and T. Tamamura: Jpn. J. Appl. Phys. **36** (1997) 4194.
17) T. Saiki, K. Nishi and M. Ohtsu: Jpn. J. Appl. Phys. **37** (1998) 1638.
18) M. Ono, K. Matsuda, T. Saiki, K. Nishi, T. Mukaiyama and M. Kuwata-Gonokami: Jpn. J. Appl. Phys. **38** (1999) L1460.
19) N. Koguchi, S. Takahashi and T. Chikyow: J. Cryst. Growth **111** (1991) 688.
20) N. Koguchi, K. Ishige and S. Takahashi: J. Vac. Sci. & Technol. B **11** (1993) 787.
21) K. Watanabe, N. Koguchi and Y. Gotoh: Jpn. J. Appl. Phys. **39** (2000) L79.
22) T. Sekiguchi and K. Sumino: Rev. Sci. Instrum. **66** (1995) 4277.
23) T. Saiki and K. Matsuda: Appl. Phys. Lett. **74** (1999) 2773.
24) M. Michel, A. Forchel and F. Faller: Appl. Phys. Lett. **70** (1997) 393.
25) C. A. Klein: J. Appl. Phys. **39** (1968) 2029.